Analysis of the impact of PCI planning on downlink throughput performance in LTE

R. Acedo-Hernández[a,*], M. Toril[a], S. Luna-Ramírez[a], I. de la Bandera[a], N. Faour[b]

[a] *Dpt. Ingeniería de Comunicaciones*
ETSI Telecomunicación, Universidad de Málaga, Campus Universitario de Teatinos, s/n
E-29071 Málaga, Spain
[b] *Optimi-Ericsson, E-29071 Málaga, Spain*

Abstract

The planning of Physical Cell Identities (PCI) has a strong impact on the performance of Long Term Evolution cellular networks. Although several PCI planning schemes have been proposed in the literature, no study has quantified the performance gains obtained by these schemes. In this paper, a comprehensive performance analysis is carried out to quantify the impact of PCI planning on user quality of service and network capacity in the downlink of LTE. First, an analytical model for the influence of PCI planning on reference signal collisions is developed. Based on this model, different PCI planning schemes are tested on a dynamic system-level simulator implementing a macrocellular scenario. During the analysis, both Voice-over-IP and full buffer services over time-synchronized and non-time synchronized networks are considered. Results show that call blocking and dropping for real-time services and user throughput for non-real time services can be significantly improved by a proper PCI plan.

Keywords: Mobile network, Long Term Evolution, physical cell identity, reference signal, throughput

*Corresponding Author: R. Acedo-Hernández, rah@ic.uma.es, +34 952136311

Email addresses: rah@ic.uma.es (R. Acedo-Hernández), mtoril@ic.uma.es (M. Toril), sluna@ic.uma.es (S. Luna-Ramírez), ibanderac@ic.uma.es (I. de la Bandera), nizar.faour@ericsson.com (N. Faour)

1. Introduction

The size and complexity of current mobile networks make it very difficult for operators to manage them. Thus, a huge effort has been made by standardization bodies and vendors to define and develop automatic network operation features [1]. As a result, the Long Term Evolution (LTE) mobile communication standard includes Self-Organizing Networks (SON) capabilities [2] [3]. SON features aim to perform planning, optimization and healing tasks with minimal human intervention.

Physical Cell Identifier (PCI) planning in LTE has been identified as an important use case for self-planning [4] [5]. A PCI (or Layer 1 identity) is a signature assigned during network planning to identify a base station in mobility functions, such as cell reselection or handover [6]. The number of PCIs is limited, which forces several base stations (or eNodeBs, eNBs) to share the same PCI. As a result, a wrong assignment of PCIs may cause that a user receives the same PCI from two different cells (problem referred to as *collision*) or a serving cell has two neighbors with the same PCI (referred to as *confusion*) [2]. Both situations prevent users from detecting cells, causing that no radio communication is possible.

At the same time, PCI defines the location in time and frequency of signaling channels, amongst which are downlink Cell-Specific Reference Signals (CRS). In the time domain, CRSs (or pilots) are transmitted in the same OFDM symbol of the frame structure in all cells. However, in the frequency domain, each cell transmits CRSs in different subcarriers depending on the value of its PCI. Thus, each cell has a specific pilot pattern corresponding to its cell identity. The number of possible pilot patterns depends on the antenna configuration, but it is always less than 6 [7], causing that CRSs of surrounding cells often collide. CRS collisions degrade Signal-to-Interference-plus-Noise Ratio (SINR) estimates, reported by the User Equipment (UE) and later used by the eNB to select the modulation and coding scheme (MCS) for downlink transmission. Thus, an improper PCI planning may give inaccurate SINR estimates, which leads to inefficient data transmission in the downlink [8].

In the literature, most research efforts on PCI planning have focused on the avoidance of collision and confusion. For this purpose, PCI planning is formulated as a graph coloring problem, which can be solved by graph-theoretic algorithms ([9] [10] [11]) or general-purpose optimization algorithms (e.g., genetic algorithms [12]). Preliminary studies considered centralized schemes [13] and later studies evaluate distributed versions [14] [15].

Both types of schemes are considered by 3GPP for LTE [16]. Distributed PCI assignment is conceived for self-configuring eNBs to support plug-and-play operation. In this approach, a centralized entity provides a list of possible PCI values, which is then restricted by the eNB by removing those reported by terminals or by neighbor eNBs through the X2 interface [17]. Alternatively, the centralized solution is based on a central entity that stores location and PCI assignment of all eNBs in the network [18]. Thus, a collision and confusion free assignment is guaranteed at the expense of an increased computational complexity, which makes it suitable only for greenfield design or infrequent re-planning processes. In [19], a decentralized method for detecting PCI conflicts based on user measurements is proposed. Recent works have extended the analysis of PCI planning to heterogeneous LTE networks, consisting of several layers, by considering collision and confusion between cells of different layers [20] [21] [22] [23] [24] [25]. Other studies (e.g., [26]) propose optimal CRS allocation patterns in the time and frequency domains. However, these schemes do not consider CRS collisions between neighbor cells nor they are compliant with LTE standard. In [27], a heuristic PCI planning algorithm is proposed to keep PCI reuse distance within certain limits while still avoiding CRS collisions in sectors of the same site. However, although LTE network performance has been well documented (e.g., in [28] [29]), to the authors' knowledge, no study has quantified the impact of PCI planning on downlink data transmission due to pilot collisions on a system level. In this work, a performance analysis is carried out to check the impact of classical PCI planning schemes on user quality of service and network capacity in the downlink of LTE. The core of the analysis is the modeling of the influence of PCI planning on CRS collisions. The proposed model is included in a dynamic system-level simulator implementing both VoIP and full buffer services, with time-synchronized and non-time synchronized schemes, in a macrocellular scenario.

The main contributions of this work are: a) a simple interference model to evaluate the impact of PCI planning on LTE downlink performance, and b) simulation results showing how much is network capacity and user throughput influenced by PCI planning for different services. The rest of the paper is organized as follows. Section 2 formulates the PCI planning problem explaining how PCI planning determines CRS collisions. Then, section 3 outlines classical PCI planning schemes proposed in the literature, for which a downlink interference model is developed in section 4. Section 5 presents the results of simulations carried out to assess the PCI planning approaches.

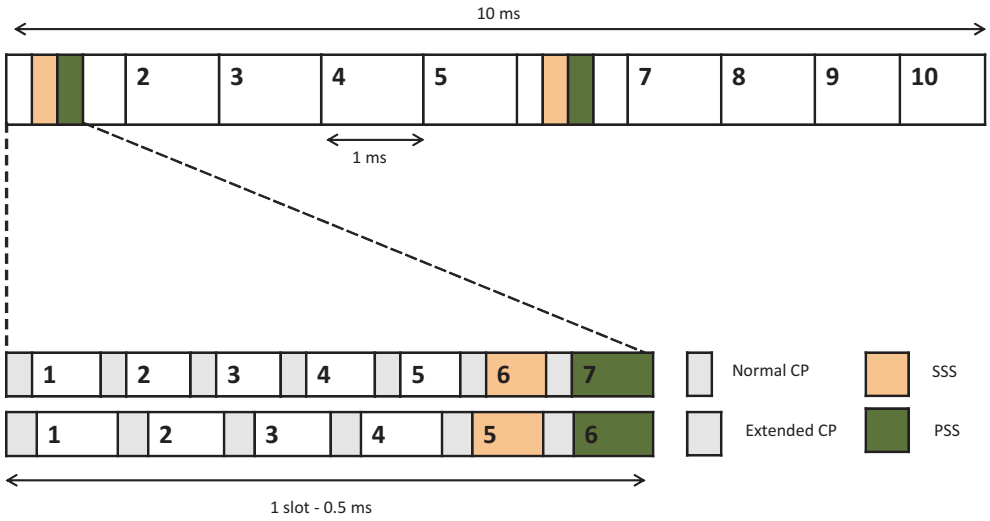

Figure 1: PSS and SSS frame and slot structure in the time domain in FDD case.

Finally, section 6 presents the concluding remarks.

2. Problem Formulation

Cell search is the first process executed by a user connecting to an LTE network. This process requires the synchronization of the radio symbols and frame user timing with that of the eNB. For this purpose, two synchronization signals are used, namely the *Primary Synchronization Signal* (PSS) and the *Secondary Synchronization Signal* (SSS), broadcasted by the eNB every 10ms [30]. PSS is used to detect the carrier frequency and the SCH (Shared Channel) symbol timing, while SSS is used to align frame timing by identifying slots within the frame. Detection of these signals not only enables synchronization, but also allows the user to obtain the PCI of the cell.
Fig. 1 shows the structure of PSS and SS frame in the time domain in the frequency division duplex (FDD) case. During cell search, the UE first finds the PSS, which is located in the last OFDM symbol of the first time slot in the first subframe (subframe 0) of a radio frame. Thus, the UE obtains the physical layer identity, ranging from 0 to 2. Then, the UE finds the SSS, which is also located in the same subframe of PSS, but in the previous symbol. From SSS, the UE obtains the physical layer cell identity group number, ranging from 0 to 167. By combining physical layer identity and cell identity

group number, the UE derives the PCI of the cell as:

$$PCI(i) = 3 * SSS(i) + PSS(i) \ , \tag{1}$$

where $SSS(i)$ and $PSS(i)$ represent the physical layer cell identity group and the physical layer identity within the physical layer cell identity group for cell i, respectively. This leads to only 504 available PCIs. Thus, there is not a unique PCI per cell, since the same PCI will be probably used more than once in the network. As a consequence, a proper assignment of PCIs to cells (referred to as *PCI plan*) should minimize local PCI conflicts by avoiding collision and confusion of PCI. Collision avoidance entails that two neighbor cells should not have the same PCI. Otherwise, a UE located in the common coverage area may not be able to decode channels from the serving base station. Confusion avoidance aims to ensure that any two cells in the network having the same PCI do not share a neighbor. In case of PCI confusion, the serving cell would not be able to identify the target cell for handover purposes [31]. In addition to avoiding collision and confusion, a proper PCI plan can increase downlink efficiency by improving channel estimates. In LTE, downlink channel estimation is based on Cell-specific Reference Signals (CRS). The PCI determines the allocation of radio resources to CRSs in a cell, which affects inter-cell interference [7]. Fig. 2 shows the CRS pattern in time and frequency for one Physical Resource Block (PRB) and Transmission Time Interval (TTI) with the normal cyclic prefix. Squares in the figure represent the different Resource Elements (REs), each consisting of the combination of a subcarrier and an OFDM symbol. Red squares correspond to REs reserved for CRSs, while white squares correspond to REs reserved for data transmission in Physical Downlink Control Channel (PDCCH), Physical Downlink Shared Channel (PDSCH), PBCH (Broadcast channel) or PMCH (Multicast channel). Note that CRSs are always transmitted in the same OFDM symbol for all PRBs in the cell, regardless of the PCI value. However, in the frequency domain, the value of the PCI in the cell defines the frequency shift of CRSs from a limited set of values, determined by computing modulo-6 of the PCI (when using one antenna port) or modulo-3 (when using two antenna ports or four antenna ports) [8]. Such a mod6 (mod3) operation is due to the arrangement of CRSs within a PRB, shown in Fig. 2, where CRSs are spaced apart by 6 (3) subcarriers in the lattice grid with one (two/four) antenna port(s) observed. In the case of four antenna ports, the reference signals from the two added antennas are sent in the following time slot (not in the same OFDM symbol) therefore, the frequency shift is the

same as in the case of two antenna ports and the location of the CRS signals also would be given by PCImod3. As a result, each cell has a specific pilot pattern based on its PCI. In this work, two antenna ports are considered, so that CRS location is given by $PCI \, mod \, 3$, which coincides with the value of PSS. For this reason, hereafter, the term PSS planning will be used to refer to those aspects of PCI planning related to CRS location. CRS location in nearby cells has a strong influence on the quality of DownLink (DL) channel estimates. As will be discussed later, CRS SINR (Signal to Interference plus Noise Ratio) depends on CRS collisions, given by the PCI value of neighbor cells. Such measurements are used to compute Channel Quality Indicators (CQI) reported by the UE, from which the eNB selects the Modulation and Coding Schemes (MCS) for PDSCH. In this work, the impact of PSS planning on channel estimation, Adaptive Modulation and Coding (AMC) and, ultimately, on DL throughput performance is evaluated.

3. PSS planning schemes

As previously mentioned, PSS allocation determines the alignment of signaling (i.e., CRSs) or data resource elements (i.e., PDSCH/PDCCH subcarriers) between neighbor cells. When assigning PSS to cells, a design choice must be made between favoring CRS $\rightarrow$ CRS interference or CRS $\rightarrow$ PDSCH/PDCCH interference. These two options lead to the planning strategies described next.

3.1. Shifted Reference Signals

By using different PSSs in adjacent cells, CRSs are allocated in different subcarriers within a PRB. Thus, in a certain subcarrier, at most, one of those adjacent cells will transmit CRSs, while the others transmit data. Fig. 3(a) shows the CRS location in three neighbor cells using a shifted CRS plan. The horizontal axis represents time (OFDM symbol) and the vertical axis denotes frequency (subcarrier). In the figure, it is assumed that the frame structure of all cells is aligned in time (synchronized network). From the figure, it can easily be deduced that the number of different PSS values is limited (i.e., 3), causing that some CRS collisions still occur with other adjacent cells.

3.2. Non-Shifted Reference Signals

Using the same PSS in adjacent cells will force alignment of CRSs, generating CRS collisions between those cells. Fig. 3(b) shows this situation for three cells.

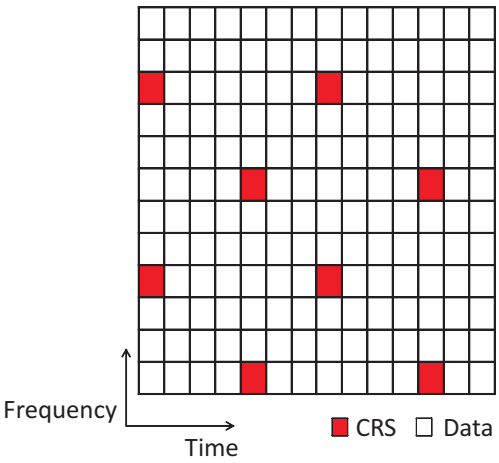

(a) 1 antenna port

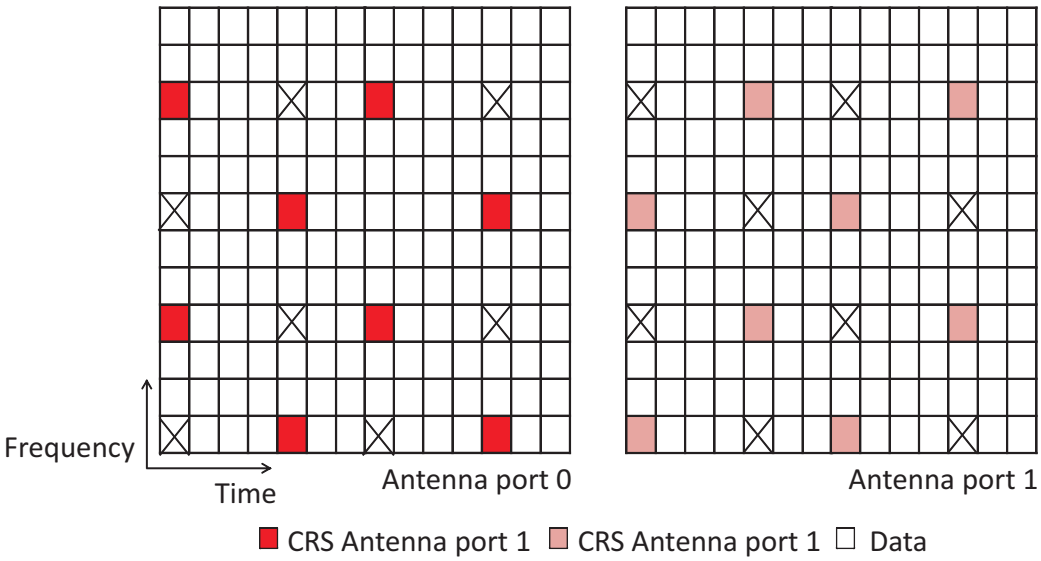

(b) 2 antenna ports

Figure 2: Cell-specific reference signal pattern in a PRB and TTI.

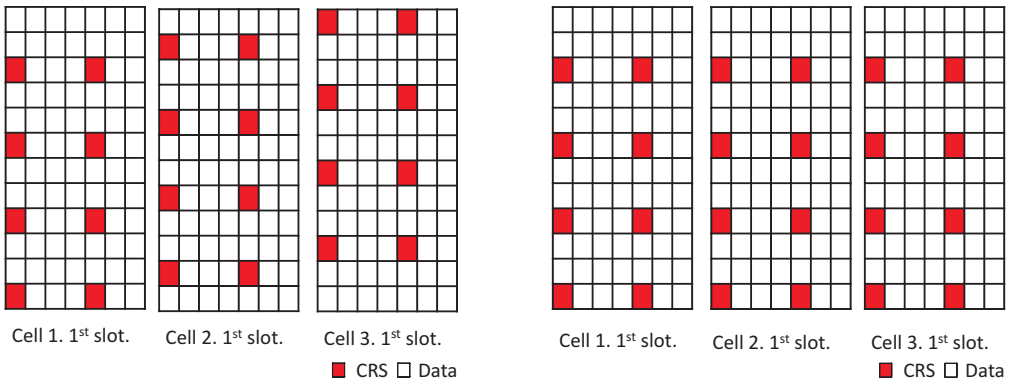

(a) Shifted CRS plan (b) Non-shifted CRS plan

Figure 3: CRS pattern in neighbor cells with different CRS plans.

4. Interference model

From the previous explanation, it can be deduced that DL interference levels are influenced by the PSS plan, apart from the propagation environment and the spatiotemporal traffic distribution. To describe such a dependency, three matrices are defined. First, an interference matrix, $I_{DL}(i, j, k)$, is built with the signal level received by user i from eNB j in each PRB k, provided that PRB k is used. Fig. 4(a) shows the structure of this matrix, whose elements depend on transmit level[1], user-dependent pathloss (including antenna gains) and frequency-selective fading (responsible for differences between PRBs). For convenience, two other matrices, $CP_{pilot}(i, j, k)$ and $CP_{data}(i, j, k)$, whose structure is shown in Fig. 4(b), are defined to evaluate the collision probability with neighbor cells. $CP_{pilot}(i, j, k)$ denotes, for a pilot RE in the kth-PRB of the serving cell of user i, the probability of colliding with interfering cell j. Similarly, $CP_{data}(i, j, k)$ reflects collision probabilities for data REs in the serving cell of user i. As will be shown later, the distinction between data and pilot REs makes analytical treatment easier. Both matrices do not only depend on the PCI of the interfering cell j, but also on that of the serving cell of user i, and hence the need for a three dimensional matrix. From these matrices, the average received interference level in pilot

[1]It is assumed here that transmit power is the same for data and pilot REs (i.e., no pilot power boosting exists).

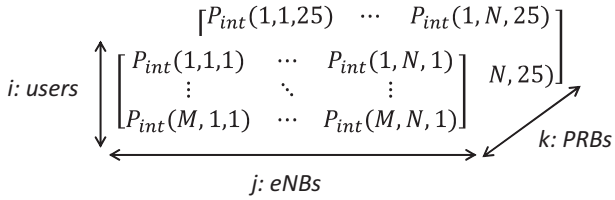

(a) Interference matrix, $I_{DL}(i,j,k)$

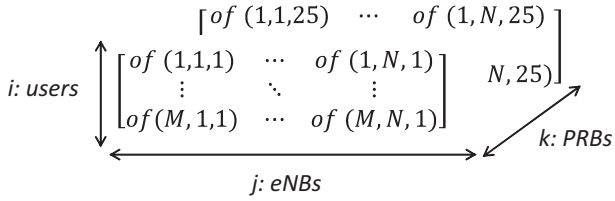

(b) Collision probability matrices, $CP_{pilot}(i,j,k)$ and $CP_{data}(i,j,k)$

Figure 4: Mathematical structures used in the interference model.

and data REs can be computed as

$$I_{pilot}(i,j,k) = I_{DL}(i,j,k) \cdot CP_{pilot}(i,j,k), \tag{2}$$

$$I_{data}(i,j,k) = I_{DL}(i,j,k) \cdot CP_{data}(i,j,k). \tag{3}$$

Note that interference level for a certain user may fluctuate, since I_{DL} changes with user mobility, and CP_{pilot} and CP_{data} depend on PRB utilization(or cell load), which changes as a result of call arrival/termination and link adaptation processes. The latter dependency of collision probabilities on cell load can be formulated as:

$$\begin{aligned} CP_{pilot}(i,j,k) &= CP_{pilot\to pilot}(i,j,k) + CP_{data\to pilot}(i,j,k) \\ &= P_{aligned\,crs}(i,j) + (1 - P_{aligned\,crs}(i,j)) \cdot L(j,k), \end{aligned} \tag{4}$$

$$\begin{aligned} CP_{data}(i,j,k) &= CP_{pilot\to data}(i,j,k) + CP_{data\to data}(i,j,k) \\ &= \left(\frac{N_{crs\,re}(1 - P_{aligned\,crs}(i,j))}{N_{data\,re}} \right) \\ &+ \left(\frac{N_{data\,re} - N_{crs\,re}(1 - P_{aligned\,crs}(i,j))}{N_{data\,re}} \right) \cdot L(j,k). \end{aligned} \tag{5}$$

where CP_{pilot} is expressed as the sum of CRS $\rightarrow$ CRS and data $\rightarrow$ CRS collissions, and CP_{pilot} as the sum of CRS $\rightarrow$ data and data $\rightarrow$ data collissions. $P_{aligned\,crs}(i,j)$ is the probability that CRSs are aligned in time and frequency between serving and interfering cell (i.e., CRS collision), $L(j,k)$ is the average load of PRB k in the interfering cell j, and $N_{data\,re}$ and $N_{crs\,re}$ are the number of data and pilot REs per PRB and time slot (i.e., 76 and 8 for 2 antenna ports [7]). In (4), it is used that the collision probability is 1 when colliding with a CRS, and $L(j,k)$ when colliding with a data RE. To derive (5), it is also used that the number of pilot-to-data collisions per PRB and time slot can be at most $N_{crs\,re}$ (out of $N_{data\,re}$). Note that $P_{aligned\,crs}(i,j)$ in (4) and (5) can take fractional values, in which case it reflects the ratio of CRSs colliding with other CRSs. For tractability, two different situations are identified, namely time-synchronized and non-time-synchronized network.

4.1. Time-synchronized network case

In a time-synchronized network, the frame structure of all base stations is time aligned, so that CRSs in all cells are transmitted in the same OFDM symbol. Thus, $P_{aligned\,crs}(i,j)$ equals 1 if serving and interfering cell have the same PSS, 0 otherwise. By substituting these values in (4), it is obtained that

$$CP_{pilot}(i,j,k) = \begin{cases} 1 & \text{if } PSS(BS_{serv}(i)) = PSS(j), \\ L(j,k) & \text{if } PSS(BS_{serv}(i)) \neq PSS(j)\ , \end{cases} \tag{6}$$

and

$$CP_{data}(i,j,k) = \begin{cases} L(j,k) & \text{if } PSS(BS_{serv}(i)) = PSS(j), \\ \frac{N_{crs\,re}}{N_{data\,re}} & +\frac{N_{data\,re}-N_{crs\,re}}{N_{data\,re}} L(j,k) \\ & \text{if } PSS(BS_{serv}(i)) \neq PSS(j)\ , \end{cases} \tag{7}$$

where $PSS(*)$ is the PSS value assigned to cell $*$ and $BS_{serv}(i)$ denotes the serving cell of user i. In (7), it has been used that, when the interfering RE is a CRS, which is in $N_{crs\,re}$ out of $N_{data\,re}$ cases, the collision probability is 1, whereas the interfering RE is a data RE, which is in $N_{data\,re} - N_{crs\,re}$ out of $N_{data\,re}$ cases, the collision probability is the cell load of the interfering cell in that particular PRB.

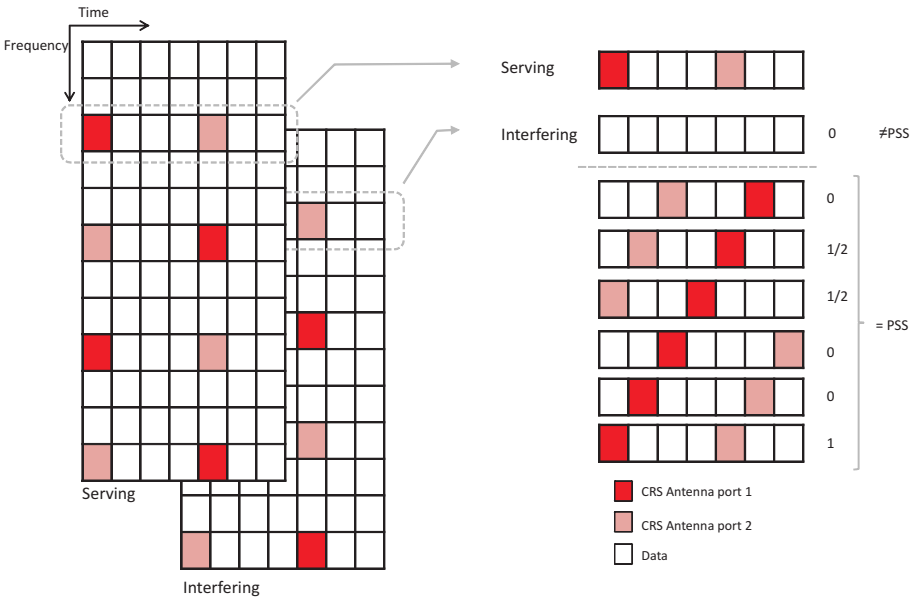

Figure 5: Possible time shifts and associated collision probabilities.

4.2. Case 2: Non-time synchronized network case

In the absence of time synchronization, the frame structure of any pair of base stations may be time shifted. Fig. 5 shows the ratio of CRSs colliding between two cells with 2 antenna ports for different time shifts, provided that CRSs are in the same subcarriers in both cells. From the values in the figure, it can be deduced that, for the considered 2x2 MIMO configuration, the average ratio of CRSs colliding in time is $\frac{1+0.5+0.5}{7} = \frac{2}{7}$. Thus, $P_{aligned\,crs}(i,j)$ is 2/7 if serving and interfering cell have the same PSS, and 0 otherwise, so that

$$CP_{pilot}(i,j,k) = \begin{cases} \frac{2}{N_s} + (1-\frac{2}{N_s})L(j,k) & \text{if } PSS(BS_{serv}(i)) = PSS(j), \\ \text{L(j,k)} & \text{if } PSS(BS_{serv}(i)) \neq PSS(j)\ , \end{cases} \quad (8)$$

$$CP_{data}(i,j,k) = \begin{cases} \frac{N_{crs\,re}(1-\frac{2}{N_s})}{N_{data\,re}} + \left(\frac{N_{data\,re}-N_{crs\,re}(1-\frac{2}{N_s})}{N_{data\,re}}\right) L(j,k) \\ \qquad \text{if } PSS(BS_{serv}(i)) = PSS(j)\ , \\ \frac{N_{crsre}}{N_{data\,re}} + \left(\frac{N_{data\,re}-N_{crs\,re}}{N_{data\,re}}\right) L(j,k) \\ \qquad \text{if } PSS(BS_{serv}(i)) \neq PSS(j)\ , \end{cases} \quad (9)$$

where N_s is the time period of pilot transmission expressed in OFDM symbols (i.e., a pilot is sent every N_s OFDM symbols in the CRS subcarrier). Collision probabilities for other antenna configurations can easily be derived following the methodology shown in Fig. 5.

4.3. Preliminary theoretical analysis

From an inspection of the previous formulas, the following conclusions can be drawn:

- In (5), it is observed that $CP_{data}(i,j,k) \approx L_{data}(i,j,k)$, regardless of the value of $P_{aligned\,crs}$, since $N_{pilot\,re}/N_{data\,re} \to 0$.

- By comparing (6) with (7) and (8) with (9), it can be observed that, in any synchronization scheme, $CP_{pilot} \neq CP_{data}$, which causes that $I_{pilot} \neq I_{data}$. Such a difference in interference levels between pilot and data REs cause that channel quality (in terms of SINR) is under- or overestimated. Specifically, if $CP_{pilot} > CP_{data}$, then $I_{pilot} > I_{data}$, $SINR_{pilot} < SINR_{data}$, and channel quality is underestimated. Thus, a too conservative AMC scheme is selected. Conversely, if $CP_{pilot} < CP_{data}$, then $I_{pilot} < I_{data}$, $SINR_{pilot} > SINR_{data}$, and channel quality is overestimated. As a result, an excessively aggressive AMC scheme is selected, which might produce many retransmissions. Both situations lead to lower DL user throughput and should be avoided.

- A similar comparison shows that the magnitude of estimation error is larger when channel quality is underestimated than when it is overestimated. For instance, in the non-time synchronized case, $CP_{pilot} - CP_{data} = 1 - L_{data} \geq 0$ if cells have different PSS (quality underestimated case), whereas $CP_{pilot} - CP_{data} \approx L_{data} - L_{data} = 0$ if cells share PSS (quality overestimated case).

- As expected, $CP_{data} \to CP_{pilot}$ as $L_{data} \to 1$, since interference is the same in data and pilot REs in a fully loaded network.

From these observations, it is expected that a proper PCI planning increases DL user throughput by reducing interference on CRSs, especially in low load scenarios. This statement is confirmed by simulation results presented in the next section.

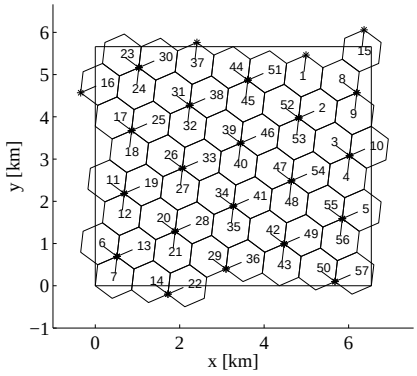

Figure 6: Simulation scenario.

5. Performance Analysis

In this section, the above-described PSS planning schemes are compared in a dynamic system level LTE simulator including the interference model described in section 4. For clarity, the analysis set-up is first introduced and results are then presented.

5.1. Analysis set-up

Simulations have been carried out with the dynamic system-level LTE simulator described in [32]. The considered macrocellular scenario, shown in Fig. 6, consists of 19 tri-sectorized sites evenly distributed in space [32]. To avoid border effects, a wrap-around technique has been used with replicas of the scenario surrounding the original one [33]. Table 1 shows the main parameters of the simulation tool. The reader is referred to [32] for a more detailed explanation of the simulation tool and the configuration parameters. Due to the large number of cases considered , the value of some simulation parameters are selected to keep the computational load within reasonable limits. Thus, time resolution is set to 100 ms and system bandwidth is set to 5 MHz. It has been checked in the most representative cases that these settings give the same relative performance difference between methods as that obtained with larger time resolution and bandwidth.

Two services are considered in the analysis: Full Buffer (FB) and Voice-over-IP (VoIP). The selection of FB service aims to check the impact of PSS planning on delay-tolerant services, which can make the most of bursty network capacity, whereas VoIP does the same for delay-sensitive low-throughput

Table 1: Simulation parameters

Cellular layout	Hexagonal grid 57 cells (3 x 19 sites)
Transmission direction	Downlink
Carrier frequency	2.0 GHz
System bandwidth	5 MHz (25 PRBs)
Frequency reuse	1
Cell radius	0.5 km
Inter Site Distance (ISD)	1.5 km
Propagation model	Okumura-Hata with wrap around Log-normal slow fading, σ = 8dB, correlation distance = 20 m Multipath fading, ETU model
Mobility model	Random direction, constant speed, 3 km/h
Service model	VoIP: Poisson traffic arrival, mean call duration: 120 s, 16 kbps Full Buffer: Transport block size exact fit to PRB allocation
Base station model	Tri-sectorized antenna, MIMO 2x2, EIRP_{max} = 43 dBm
Scheduler	Proportional Fair Resolution: 1PRB
Power control	Equal transmit power per PRB
Link Adaptation	CQI based
RRM features	Directed Retry, Handover, Call access control
HO parameter settings	TimetoTrigger = 100 ms HO margin=3dB
Traffic distribution	Uniform and non-uniform spatial distribution
Dropped call model	Radiolinktimeout=1 sec
Time resolution	100 TTI (100 ms)
Simulated network time	1 hour (per PCI plan)

services. An FB user will always make use of the available network radio resources, whereas a VoIP user transmit packets with fixed size and frequency (40 bytes every 20 ms, i.e., 16 kbps). Both services are simulated independently, since the focus of this work is on the impact on PSS planning on different types of services, and not on the scheduler. Likewise, both uniform and non-uniform user spatial distribution are evaluated. In both cases, user population is configured so as to achieve a certain value of overall PRB utilization in the scenario (in this work, either 30% or 80%). A MIMO (Multiple Input Multiple Output) 2x2 configuration is assumed. Thus, the number of different PSS codes (and, hence, of CRS shifts) is 3. Five different PSS planning schemes are considered:

1) Scheme 0 (Ideal): A first scheme assumes perfect PSS planning, so that CRS $\rightarrow$ CRS collisions do not take place. Interference on CRSs from other cells is originated only by data REs. Thus, CRS SINR depends on PRB utilization of interfering cells. This scheme is considered as a benchmark, and it is the typical configuration in most system-level simulators, where PCI planning is neglected.

2) Scheme 1a ($\neq$ PSS, nTS): A PSS plan is built by a shifted PSS strategy ($\neq$

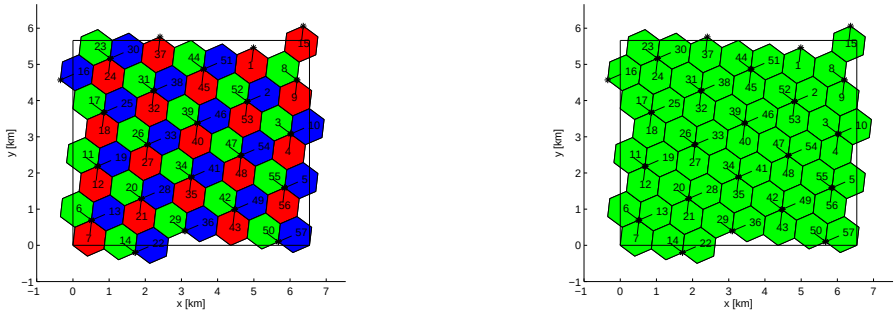

(a) Shifted PSS schemes (Schemes 1a/1b).

(b) Non-shifted PSS schemes (Schemes 2a/2b).

Figure 7: PSS plans in the scenario.

PSS) in a non-time synchronized network (nTS). As the number of possible frequency shifts is 3, some CRS collisions occur. Thus, interference on CRSs comes from pilot or data subcarriers depending on the interfering cell. Fig. 7(a) shows the best PSS plan to reduce CRS collisions. Each color represents one of the 3 different shifts (i.e., PSS codes). Due to the symmetry of the scenario, the PSS plan is built by reusing the 3 shifts on a per-site basis. Note that, in this scheme, CRS $\rightarrow$ CRS collisions are unlikely due to the lack of synchronization between cells, and CRS $\rightarrow$ data collisions are the most likely.

3) Scheme 1b ($\neq$ PSS, TS): A PSS plan is built by a shifted PSS strategy in a time synchronized network. In this case, PSS plan is still that of Fig. 7(a). However, CRSs are time aligned, and, consequently, CRSs collisions are more likely.

4) Scheme 2a (=PSS, nTS): PSS plan is built by aligning CRSs in a non-time synchronized network. The resulting PSS plan is shown in Fig. 7(b), where it is observed that all cells have the same PSS value. Nonetheless, CRS collisions are still unlikely due to the lack of synchronization.

5) Scheme 2b (=PSS, TS): A PSS plan is built by aligning CRSs in a time synchronized network. In this case, CRS collisions occur frequently as all BSs share the same location of CRSs both in time and frequency. This scheme represents the worst case.

Eight use cases are defined, consisting of combinations of service (FB or VoIP), network load (30% or 80%) and spatial traffic distribution (uniform or non-uniform). For a fair comparison of methods, network load is controlled by user population, which is kept the same for all schemes. Note that the load of a cell is 100% as long as one FB user is connected. In this work, a value X% of network load is achieved for the FB service by forcing that only X% of radio resources can be used in every cell. Such a constraint is imposed on the scheduler, which assigns exactly X% of resource elements in every PRB, provided that there is at least one user in the cell. By distributing users among PRBs in each cell, load (and, hence, interference) is the same across PRBs. It should be pointed out that the exact load will vary between 25-30% for low load and 70-80% for high load depending on the scheme. Note that, even if the user population is kept the same for all schemes (for a fair comparison of network capacity), network load might not be exactly the same due to the impact of interference on link efficiency (i.e., number of PRBs per connection), access control (i.e., number of blocked calls) and connection quality (i.e., number of dropped calls). On the other hand, in the uniform case, all the cells have the same maximum occupancy factor value, whereas, in the non-uniform case, an irregular traffic distribution is generated by setting the maximum allowed load to be different in each cell of the scenario (while still keeping user population unaltered). In the latter case, the PRB utilization of each cell will be different, but the average network load is still the same as in the uniform case. The normalized spatial load distribution in the irregular case is represented in Fig. 8. For each use case, the 5 PSS schemes are simulated. Performance assessment is based on several key performance indicators. For FB service, indicators are: a) as a measure of connection quality , DL CRS SINR for cell-edge and average user, defined as the 5%-tile and the median value of the CRS SINR distribution; b) as a measure of link efficiency, the Channel Quality Indicator (CQI) distribution; c) as a measure of user quality of service and fairness, cell-edge and average user throughput; and d) as a measure of network capacity, average DL cell throughput. For VoIP, indicators are: a) as a measure of network capacity, Call Blocking Ratio (CBR), defined as the ratio between blocked and offered calls, and b) as a measure of quality of service, Call Dropping Ratio (CDR), defined as the ratio between dropped and carried calls. In this work, a call is dropped if no resources are assigned to the user or a bad SINR is experienced for more than $1s$. The simulated network time (1 hour) proves to be enough to obtain reliable estimates of these indicators once aggregated for the whole

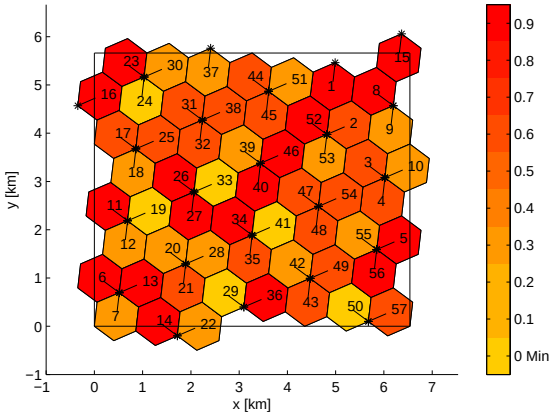

Figure 8: Non-uniform load distribution.

scenario. Thus, confidence intervals for measurements are not shown in the analysis.

5.2. Analysis Results

For clarity, results for FB service are presented first and those of VoIP are described later. In both cases, the analysis is first focused on the results with uniform spatial traffic distribution and then on the impact of uneven spatial traffic distribution.

5.2.1. Full Buffer Service

The analysis begins with the comparison of the different PSS planning approaches with uniform spatial distribution. Fig. 9(a) shows the DL CRS SINR distribution with FB users and a low uniform network load (i.e., PRB utilization of 30%). As expected, Scheme 0 (ideal case, where no CRS collisions exist) obtains the highest SINR values. In contrast, PSS plans with aligned pilots (Schemes 2a and 2b) achieve the worst performance. Likewise, non-time synchronized plans (Schemes 1a and 2a) outperform their time-synchronized counterparts (1b and 2b, respectively). It can thus be concluded that a proper PSS planning can avoid most CRS collisions in the non-time synchronized case, which is evident from the small difference between Scheme 0 and Scheme 1a. More importantly, the shape of the curves is maintained, so that distributions of real schemes are just shifted versions of that of the ideal scheme. From this result, it can be inferred that all

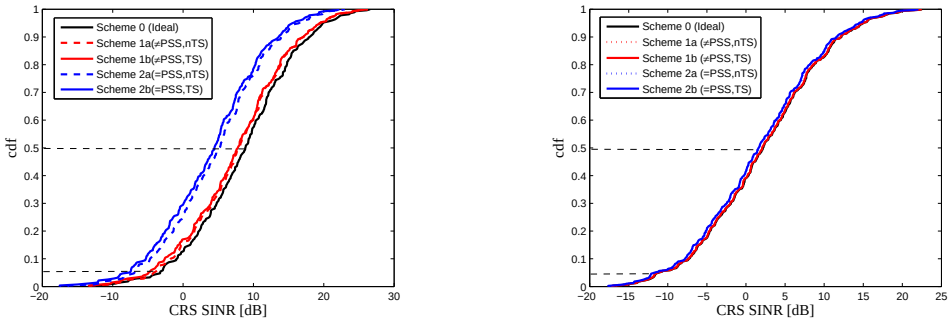

(a) Low load (L=30%) (b) High load (L=80%)

Figure 9: SINR distribution for downlink reference signals for FB service and uniform traffic.

Table 2: Downlink CRS SINR with low uniform load (L=30%).

Scheme	S0	S1a	S1b	S2a	S2b
DL CRS SINR (5%-tile) [dB]	-3.26	-3.86	-4.64	-6.87	-8.61
DL CRS SINR (50%-tile) [dB]	9.01	7.98	7.78	5.54	3.86

users (either cell center or cell edge) experience roughly the same decrease in CRS SINR values due to bad PSS planning. Such an impairment can easily be quantified by a single value denoting the magnitude of the shift, which can be interpreted as an increase of the average interference level. A more detailed analysis shows that this SINR impairment factor for the worst case (Scheme 2b) compared to the ideal case (Scheme 0) proves to be $10\log L$, where L is the average network load. To backup this statement, Table 2 shows the values of 5%-tile (i.e., cell-edge) and median DL CRS SINR. It is observed that the difference in DL SINR on cell edge between the worst and the best PSS planning scheme is 5.15 dB ($\approx 10\log 0.3$). The same holds true for the median SINR value. For high network load (i.e., 80%), all PSS schemes perform approximately the same, as shown in Fig. 9(b). Due to such a high PRB utilization, the probability of a CRS in a cell colliding with a data subcarrier in its neighbors approaches that of colliding with a CRS (equal to 1). Table 3 confirms DL SINR estimation for different PSS plans. The difference between the worst and best schemes is now only 0.65 dB ($\approx 10\log 0.8$).

Fig. 10(a) and 10(b) show the CQI distribution obtained for low and high uniform network loads, respectively. For low network load, the average CQI

Table 3: Downlink CRS SINR with high uniform load (L=80%).

	S0	S1a	S1b	S2a	S2b
DL CRS SINR (5%-tile) [dB]	-11.11	-11.10	-11.02	-12.08	-12.14
DL CRS SINR (50%-tile) [dB]	2.23	2.065	1.98	1.64	1.58

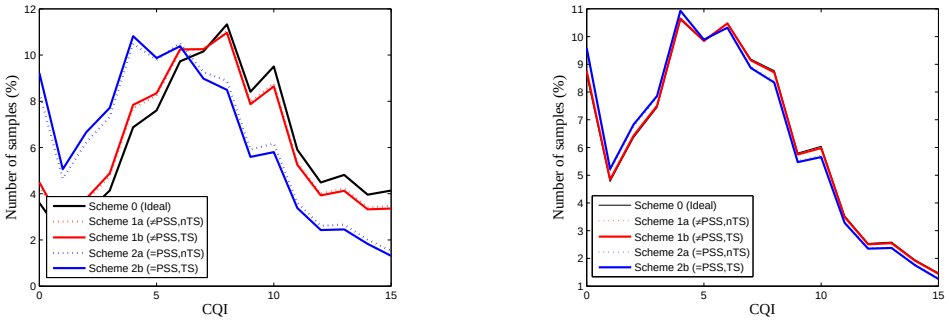

(a) Low load (L=30%) (b) High load (L=80%)

Figure 10: CQI distribution for FB service and uniform network load.

value degrades from 9.4 for Scheme 0 up to 7.5 for Scheme 2b. Note that the number of samples with the largest value (CQI = 15) in Scheme 0, 1a and 1b is larger than in Scheme 2a and 2b. Thus, the most effective AMC schemes are rarely used in the latter schemes, which should lead to lower peak throughput for cell center users. In contrast, in Fig 10(b), it is shown that, for high network load, all schemes show the same CQI distribution. When comparing Fig. 10(a) and Fig 10(b), it is observed that CQI values are smaller (worse) for all schemes for high network load as a result of a higher PRB utilization and, consequently, a higher interference. Thus, more robust AMC schemes must be selected to compensate for the lower SINR values.

Fig. 11(a) depicts DL user throughput distribution for low uniform network load. User throughput ranges from 0 to 6.99 Mbps ($\approx$ 1 Mbps/PRB $\cdot$ 25 PRBs $\cdot$ 0.3 network load) for all schemes, and, again, Schemes 1a and 1b perform better than 2a and 2b, and similar to an ideal PSS plan (i.e. Scheme 0). More specifically, Scheme 2b experiences a 48% decrease (i.e, from 588 to 300 kbps) in cell-edge user throughput (i.e. 5%-tile), while a 31% decrease (i.e., from 3.33 to 2.27 Mbps) is observed for the median user (50%-tile), compared to Scheme 0. This suggests that PCI planning has a larger impact on cell-edge and average users than on best (cell-center) users, where the throughput losses are about 9.67% (i.e, from 6.95 Mbps to 6.281

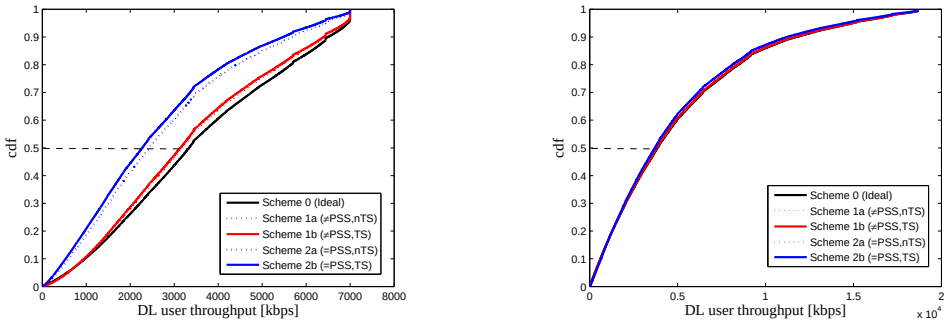

(a) Low load (L=30%) (b) High load (L=80%)

Figure 11: DL user throughput for FB service and uniform network load.

Table 4: DL user throughput with low uniform load (L=30%).

	S0	S1a	S1b	S2a	S2b
DL THRU (5%-tile) [kbps]	588	579	561	344	297
DL THRU (50%-tile) [Mbps]	3.33	3.18	3.14	2.41	2.27
DL THRU (100%-tile) [Mbps]	6.99	6.97	6.9	6.87	6.82

Mbps). User throughput loss caused by an improper PCI planning comes from the use of excessively robust AMC schemes, which are selected because channel quality is subestimated due to pilot collisions. In contrast, Fig. 11(b) shows that the impact of PSS planning on user throughput distribution is negligible for a high network load. In this case, user throughput ranges from 0 to 18.68Mbps ($\approx$ 1 Mbps/PRB $\cdot$ 25 PRBs $\cdot$ 0.8 network load). More specifically, Table 5 shows that cell-edge and average users experience a throughput decrease of only 47 kbps and 170 kbps, respectively (i.e., 13.82% and 4.4%). Nonetheless, it can still be concluded that user throughput decreases with aligned schemes.

Differences in user throughput translate into differences in cell throughput. Fig 12(a) and 12(b) show the DL cell throughput distribution for low and high network load, respectively. Note that, besides by the PSS plan, cell

Table 5: DL user throughput with high uniform load (L=80%).

	S0	S1a	S1b	S2a	S2b
DL THRU (5%-tile) [kbps]	340	338	305	303	293
DL THRU (50%-tile) [Mbps]	3.87	3.83	3.83	3.71	3.70
DL THRU (100%-tile) [Mbps]	18.68	18.68	18.67	18.65	18.6

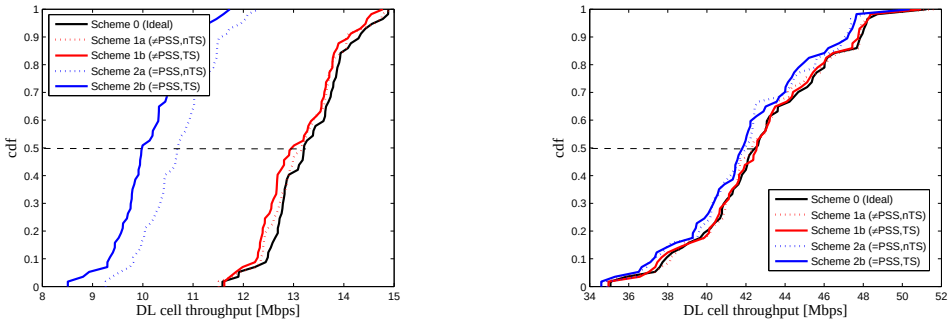

(a) Low load (L=30%) (b) High load (L=80%)

Figure 12: DL cell throughput.

Table 6: DL cell throughput with low uniform load (L=30%).

	S0	S1a	S1b	S2a	S2b
DL cell THRU (50%-tile) [Mbps]	13.21	13.17	13.01	10.7	9.99

throughput changes during simulation due to the call arrival and user mobility random processes. Thus, the analysis is hereafter focused on average cell throughput. Fig. 12(a) shows DL cell throughput for low network load. It is observed that average cell throughput decreases by up to 24.3% when Scheme 2b is compared to Scheme 0. Likewise, Fig 12(b) shows how average cell throughput only decreases by 1.61% for high network load.

The next experiment shows the impact of the spatial traffic distribution on the performance of PSS plans for FB service. This is done by comparing the results with uniform and non-uniform load distribution. Recall that, in the non-uniform case, the maximum allowed PRB utilization is fixed to a different value in each cell of the scenario. For brevity, only low traffic conditions are simulated, as it has been shown before that all PSS plans perform the same with large network load.

Fig 13 presents the values of the different network performance indicators with even and uneven load distribution. Only Schemes 0 and 2b are shown in the figure, as these can be considered as upper and lower bounds for the

Table 7: DL cell throughput with high uniform load (L=80%).

	S0	S1a	S1b	S2a	S2b
DL cell THRU (50%) [Mbps]	42.67	42.58	42.41	42.22	41.98

performance of PSS plans. In Fig. 13(a) and 13(b), it is observed that Scheme 2b has identical SINR and CQI distribution for uniform and non-uniform distribution. This result was expected as collisions on pilots are only due to other cells's pilots, whose usage does not depend on the traffic pattern or load factor. Even for the ideal PSS plan with perfectly staggered pilots (Scheme 0), the differences between non-uniform and uniform traffic are really small. Such differences are stochastic noise due to changes in cell loads caused by short time intervals without users in a cell. It can thus be concluded that the influence of spatial distribution on SINR and CQI is negligible. This is not the case for user and cell throughput, where large differences are observed. Fig 13(c) shows a larger spread of user throughput values with non-uniform traffic. In particular, maximum user throughput is 14 Mbps with non-uniform traffic and only 7 Mbps for uniform traffic. Note that user throughput is proportional to the PRB utilization factor, which is the same for all cells in the uniform case but different for each cell in the non-uniform case. Such variability is translated into a wider range of possible throughput values, which causes that the overall peak user throughput increases and cell-edge user throughput decreases with uneven traffic distribution. A closer look on the figure reveals that, for non-uniform traffic, the overall cell-edge user throughput with Scheme 0 is 43.3% larger than with Scheme 2b (i.e., 295 vs 167 kbps), which is less than the difference with uniform traffic (48%). Fig. 13(d) shows cell throughput distribution with both traffic patterns. Cell throughputs are calculated by aggregating individual user throughputs, so that a larger spread out is expected. In this case, the average cell throughput with Scheme 0 is 26.24% larger than with Scheme 2b (i.e., 15.3 vs 11.3 Mbps), which is larger than the difference with uniform traffic (24.3%).

5.2.2. VoIP

The analysis of VoIP service is restricted to the uniform traffic case. Note that VoIP traffic generation is configured through user population and call arrival rates (instead of through PRB utilization, as in the FB case). Thus, PRB utilization in VoIP cases varies with time, causing that stochastic variations in performance indicators are larger for these cases. Figures 14(a) and 14(b) show CBR and CDR for all PSS planning schemes with low and high network load, respectively. In terms of connection quality, Scheme 2b shows the largest (worst) CDR values. In particular, for this scheme, CDR is 4.2% and 7.02% for low and high load, compared to 0% and 5.1% for Scheme 1a. As shown before, Schemes 2a and 2b subestimate channel quality, so that

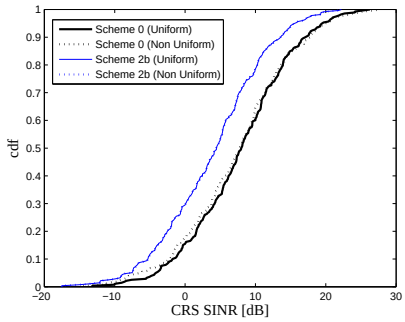

(a) DL CRS SINR

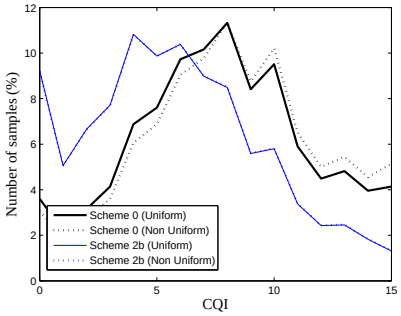

(b) CQI

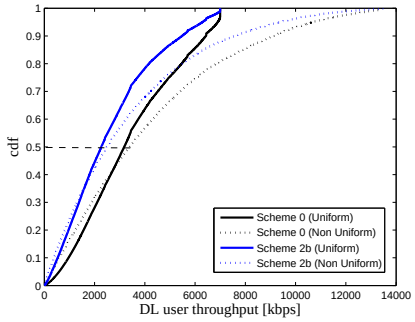

(c) DL user throughput

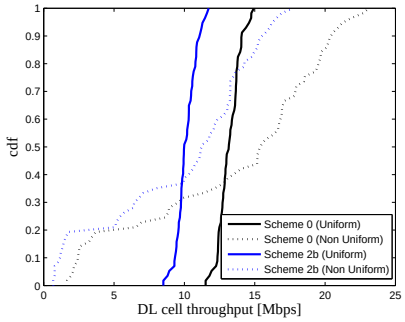

(d) DL cell throughput

Figure 13: Network performance with uniform and non-uniform spatial traffic distribution for FB service.

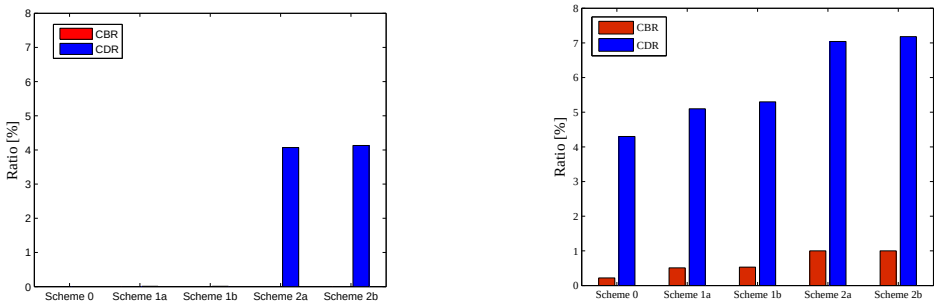

(a) Low load scenario

(b) High load scenario

Figure 14: Network performance for VoIP service with different average network load.

more robust modulations are used and PRB utilization is higher, causing call blocking and dropping due to lack of resources. A more detailed analysis (not shown here) proves that, for the same user population, the average network load varies from 90% (Scheme 2b) to 70% (Scheme 0) with high load conditions. Similarly to FB service, CDR or CBR differences between schemes in VoIP are smaller for large network load, compared to differences with low load conditions. From these results, it can be concluded that shifted-CRS schemes clearly outperform aligned CRS schemes also for VoIP service.

6. Conclusions

In this paper, a comprehensive performance analysis of the impact of PSS planning on LTE downlink performance has been carried out. For this purpose, a dynamic system-level LTE simulator has been used. The analysis has considered different services and network load conditions. Simulation results show that the impact of PSS planning is larger in lightly loaded networks, whereas it is negligible in fully loaded networks. Likewise, in the considered macrocellular scenario, a proper PSS planning with staggered reference signals ensure near-optimal performance even for time synchronized networks. In contrast, full alignment of reference symbols can lead to a decrease in average DL user throughput and DL cell throughput for FB service by 31% and 24.7% respectively, and an increase in dropped call ratio for VoIP service by up 4.2%, compared to an optimal case (Scheme 0).

Acknowledgement

This work has been funded by the Spanish Ministry of Economy and Competitiveness (TIN2012-36455) and Optimi-Ericsson, Agencia IDEA (Consejería de Ciencia, Innovación y Empresa, Junta de Andalucía , ref. 59288) and FEDER. The authors would like to thank Carlos Úbeda, R&D System Developer in Ericsson, for their valuable comments and suggestions to improve the quality of this paper.

References

[1] NGMN, Next generation mobile networks beyond HSPA & EVDO v3.0, Technical Report, 2006.

[2] J. Ramiro, Self-Organizing Networks: Self-Planning, Self-Optimization and Self-Healing for GSM, UMTS and LTE, John Wiley & Sons, 2011.

[3] S. Hamalainen, H. Sanneck, C. Sartori, LTE Self-Organising Networks (SON): Network Management Automation for Operational Efficiency, John Wiley & Sons, 2012.

[4] G. Americas, The benefits of SON in LTE: Self-Optimizing and Self-Organizing Networks, Technical Report, 3G Americas, 2009.

[5] 3rd Generation Parthnership Project, TR 36.902 V9.3.1; Technical Specification Group Radio Access Network; Evolved Universal Terrestrial Radio Access Network (E-UTRAN); Self-Configuring and Self-Optimizing Network (SON) Use Cases and Solutions (Release 9), Technical Report, 2011.

[6] 3rd Generation Parthnership Project, TR 36.211 V11.2.0; Technical Specification Group Radio Access Network; Evolved Universal Terrestrial Radio Access Network (E-UTRA); Physical Channel and Modulation (Release 11), Technical Report, 2013.

[7] S. Sesia, I. Toufik, M. Baker, LTE: The UMTS Long Term Evolution, From Theory to Practice, Wiley, 2009.

[8] D. M. J. Zyren, Overview of the 3GPP Long Term Evolution Physical Layer, Technical Report, White paper, Freescale Semiconductor, 2007.

[9] T. Bandh, G. Carle, H. Sanneck, Graph coloring based Physical-Cell-ID assignment for LTE networks, International Conference on Wireless Communications and Mobile Computing (2009) pp. 116–120.

[10] F. Ahmed, O. Tirkkonen, M. Peltomki, M. A. Juha-Matti Koljonen Chia-Hao Yu, Distributed graph Coloring for Self-Organization in lte networks, Journal of Electrical and Computer Engineering (2010).

[11] H. Xu, X. W. Zhou, Y. Li, Model of hypergraph colouring for Self-configuration in LTE Networks, International Conference on Information Management, Innovation Management and Industrial Engineering (ICIII) (2011).

[12] H. Sun, N. Li, Y. Chen, J. Dong, N. Liu, Y. Han, W. Liu, A method of PCI planning in LTE based on genetic algorithm, Progress In Electromagnetics Research Symposium, (2012) pp. 19–23.

[13] Y. Liu, W. Li, H. Zhang, L.Yu, Distributed PCI assignment in LTE based on consultation mechanism, in: Wireless Communications Networking and Mobile Computing (WiCOM), (2010), pp. 1–4.

[14] Y. Liu, W. Li, H. Zhang, W. Lu, Graph based automatic centralized PCI assignment in LTE, in: IEEE Symposium on Computers and Communications (ISCC), (2010), pp. 919 –921.

[15] Y. Wei, M. Peng, W. Wang, S. Min, J. M. Jiang, Y. Huang, Automatic Distributing Schemes of Physical Cell Identity for Self-Organizing Networks, International Journal of Distributed Sensor Networks (2012).

[16] 3rd Generation Parthnership Project, TS 36.300 V. 10.9.0; Evolved Universal Terrestrial Radio Access (E-UTRA) and Evolved Universal Terrestrial Radio Access Network (E-UTRAN); Overall description; Stage 2 (Release 10), 2013., Technical Report, 2013.

[17] 3rd Generation Parthnership Project, 3GPP TSG-RAN WG3 metting # 59, r3-080376, SON Use Case: Cell Phy_ID Automated Configuration, 2008.

[18] 3rd Generation Parthnership Project, 3GPP TSG-RAN WG3 metting # 59, R3-080812, Solution(s) to the 336.902 Automated Configuration of Physical Cell Identity Use Case, 2008.

[19] M. Amirijoo, P. Frenger, F. Gunnarsson, H.Kallin, J. Moe, K. Zetterberg, Neighbor Cell Relation List and Physical Cell Identity Self-Organization in LTE, in: IEE Interference Conference Communications Workshops (ICC), (2008), pp. 37–41.

[20] X. Zhan, D. Zhou, Z. Xiao, E. Liu, J. Zhang, A. A. Glasunov, Dynamic Group PCI Assignment Scheme, in: 7th International Conference on Wireless and Mobile Communication, ICWMC, (2011).

[21] T. Wu, L. Rui, A. Xiong, S. Guo, An Automation PCI Allocation Method for eNodeB and Home eNodeB Cell, in: 6th International Conference on IEEE Wireless Communications Networking and Mobile Computing (WiCOM), (2010).

[22] Y. Wu, H. Jiang, Y. Wu, D. Zhang, Physical Cell Identity Self-Organization for Home eNodeB Deployment in LTE, in: 6th International Conference on Wireless Communications Networking and Mobile Computing (WiCOM), (2010), pp. 1–6.

[23] A. Zahran, Extended Synchronization Signals for eliminating PCI confusion in heterogeneous LTE, in: IEEE Wireless Communications and Networking Conference (WCNC), (2012), pp. 2588–2592.

[24] J. Lim, H. Daehyoung, Management of Neighbor Cell lists and Physical Cell Identifiers in Self-Organizing heterogeneous networks, Journal of Communications and Networks 13 (2011) pp. 367–376.

[25] M. Krichen, D. Barth, O. Marce, Performances evaluation of different algorithms for PCIs Self Configuration in LTE, in: 18th IEEE International Conference on Networks (ICON), (2012), pp. 197–203.

[26] M. Simko, P. Diniz, Q. Wang, M. Rupp, Adaptive Pilot-Symbol Patterns for MIMO OFDM Systems, IEEE Transactions on Wireless Communications 12 (2013) pp. 4705–4715.

[27] H. Vadada, LTE PCI planning, 2011. Retrieved April 2, 2014 from: http://www.telecom-cloud.net/wp-content/uploads/2010/09/PCI-Planning-for-LTE.pdf.

[28] A. Elnashar, M. El-Saidny, Looking at LTE in Practice: A Performance Analysis of the LTE System Based on Field Test Results, Vehicular Technology Magazine, IEEE 8 (2013) pp. 81–92.

[29] J.-B. Landre, Z. E. Rawas, R. Visoz, LTE performance assessment : Prediction versus field measurements, in: IEEE 24th International Symposium on Personal Indoor and Mobile Radio Communications (PIMRC), (2013), pp. 2866–2870.

[30] H. Kavlak, H. Ilk, PCI planning strategies for Long Term Evolution networks, in: Proc. 2012 International Conference on Networking, (2012), IFIP'12, pp. 151–156.

[31] J. Song, T. Ma, P. Pietzuch, Towards Automated verification of autonomous networks: A case study in Self-Configuration, in: 8th IEEE International Conference on Pervasive Computing and Communications Workshops (PERCOM Workshops), (2010), pp. 582 –587.

[32] P. Muñoz, I. de la Bandera, F. Ruiz, S. Luna-Ramírez, R. Barco, M. Toril, P. Lázaro, J. Rodríguez, Computationally-Efficient design of a Dynamic System-Level LTE simulator, INTL Journal of Electronics and Telecommunications 57 (2011) pp. 347–358.

[33] T. Hytnen, Optimal wrap-around network simulation, Helsinki University of Technology Institute of Mathematics: Research Reports (2001).